

EFFECT OF CALCINATION TEMPERATURE ON THE PHYSICOCHEMICAL PROPERTIES OF MOV OXIDES PREPARED VIA REFLUX METHOD

Tan Yee Wean, Irmawati Ramli*, Taufiq-Yap Yun Hin

Department of Chemistry, Faculty of Science, Universiti Putra Malaysia, 43400 Serdang, Selangor Darul Ehsan.

**Corresponding authors email: tanyeeewan@yahoo.com ; irmawati@science.upm.edu.my*

Key words: Mo-V-O catalysts, reflux, selective oxidation of propane, TPR.

Abstract

In this study, MoV mixed oxides with a molar ratio of 10:3 were prepared by reflux method. The samples were subjected to various calcination temperatures in order to investigate the physicochemical properties of the oxide affected by the parameter. Samples were characterised by XRD, TG/DTA, BET surface area, SEM and TPR. By imposing various calcination temperatures, phase evolutions were observed. However, these changes do not significantly affect the morphology, surface area, particle size and reducibility of the oxide. Still, the best calcination temperature can be chosen to arrive at the effective catalyst necessary for the desired catalytic reaction.

Abstrak

Dalam kajian ini, oksida campuran MoV dengan nisbah molar 10:3 telah disediakan dengan kaedah refluks. Sampel-sampel tersebut dikalsin pada pelbagai suhu untuk mengkaji sifat fizikal dan kimia oksida yang dipengaruhi oleh parameter itu. Sampel-sampel dicirikan dengan belauan sinar X, analisis termogravimetri, kaedah pengukuran luas permukaan BET, pengimbasan mikroskopi elektron dan penurunan dengan suhu terprogram. Dengan menjalankan pengkalsinan pelbagai suhu, evolusi fasa diperhatikan. Walau bagaimanapun, pembolehubah ini tidak menunjukkan kesan ketara pada morfologi, luas permukaan, saiz dan penurunan oksida. Walau begitu, suhu pengkalsinan terbaik dapat dipilih untuk mendapatkan mangkin yang berkesan untuk tindak balas yang dikehendaki.

Introduction

Propane selective oxidation is one of the recent challenges in selective oxidation field. A catalyst for propane selective oxidation to acrylic acid has attracted much attention recently. However, researchers face difficulty in the development of such catalyst at an acceptable cost. This study contributes to the development of such catalysts at a low cost for industrial scale production. A detailed research and careful control of various synthesis factors are required for the production of such catalysts.

Mo-V-O based catalysts have been claimed as the active and selective catalysts in the reaction. The oxides are usually prepared by employing hydrothermal method as reported by Ueda *et al.* [1], where they successfully achieved the formation of single hexagonal phased and single orthorhombic phased MoV mixed oxide. This method however, is very exclusive and is only applicable at lab-scale synthesis. The scale-up production of the catalysts is very expensive thus almost impossible. Therefore, it is the desire of our work to synthesis active and selective catalyst using a more conventional method. The method chosen is the reflux method. The solid obtained from this route will be subjected to various calcination temperatures in order to study the physicochemical properties of the sample. This study aim to the development of such catalysts at a low cost for industrial scale production.

Experimental

0.010 moles of ammonium heptamolybdate tetrahydrate were dissolved in 80 cm³ of deionised water to form a clear solution. 0.021 moles of vanadium sulphate were dissolved in 20 cm³ deionised water to obtain a clear blue solution. The number of moles of the starting materials corresponds to the molar atomic ratio of Mo:V of 10:3 [5]. The two solutions were mixed together and were refluxed for an hour followed by ageing for 1 hour. Then, the mixture was heated below 333 K until it becomes pasty textured. The samples were later dried in a dessicator in which, upon drying were grounded into powder form. The precursor powders were then

characterised by X-ray diffraction using a Shidmazu Model XRD-6000 Diffractometer and Thermal Gravimetry/ Differential Thermal Analysis (TG/ DTA) by using Mettler Toledo Model 990 instrument, which measures mass changes when temperature increases. The precursors were heat treated in N_2 flow at 573 K, 623 K, 673 K, 723 K and 773 K for 2 hours [1,4,5,6]. These samples were denoted as MoV_{573} , MoV_{623} , MoV_{673} , MoV_{723} and MoV_{773} , respectively. The oxides were further characterised by nitrogen gas adsorption at 77 K to measure the BET total surface area. XRD and Scanning Electron Microscopy (SEM) analysis were also conducted. Samples were then subjected to Temperature Programmed Reduction (TPR) to study the amount of removable oxygen species.

Results and Discussion

X-Ray Diffraction of Precursor

The XRD patterns of the precursor are shown in Figure 1. There are some intense peaks observed at lower range. The precursor is multiphasic with the presence of $V_{0.12}Mo_{0.88}O_{2.94}$ hexagonal and $MoO_3 \cdot 0.5H_2O$ monoclinic. Other phases could not be ruled out.

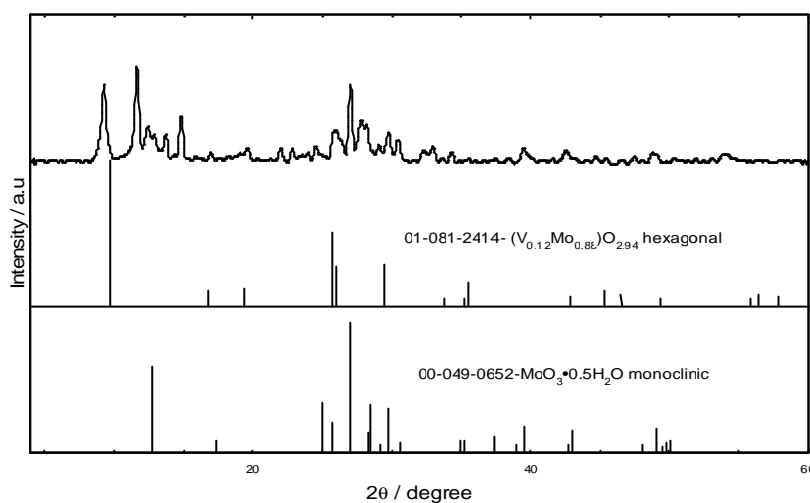


Figure 1: XRD diffractogram of precursor

Thermal Gravimetry Analysis of Precursor

Thermal Gravimetry /Differential Thermal Gravimetry (TG/DTA) were conducted for the precursor in order to determine the thermal behaviour of the samples. Figure 2 shows the TG/DTA thermograms for the precursor.

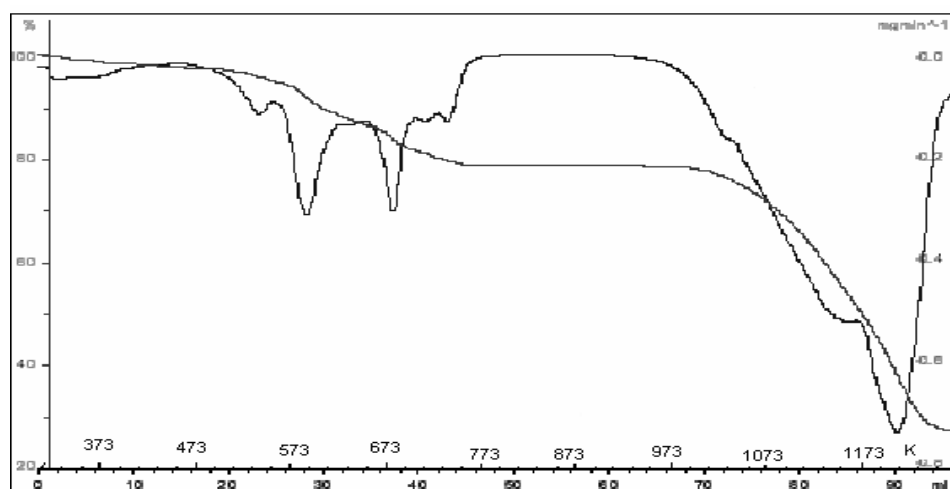


Figure 2: TG/DTA thermograms of precursor

First decomposition was observed at 343 K, corresponding to the removal of physisorbed water from the samples. Between 473 K and 773 K, another weight loss occurred corresponding to the elimination of ammonium group and water trapped in the lattice of the samples. There is no weight change in the temperature range between 773 and 973K. However, above 973 K a huge endotherm is observed, probably due to phase changes.

X-Ray Diffraction of calcined samples

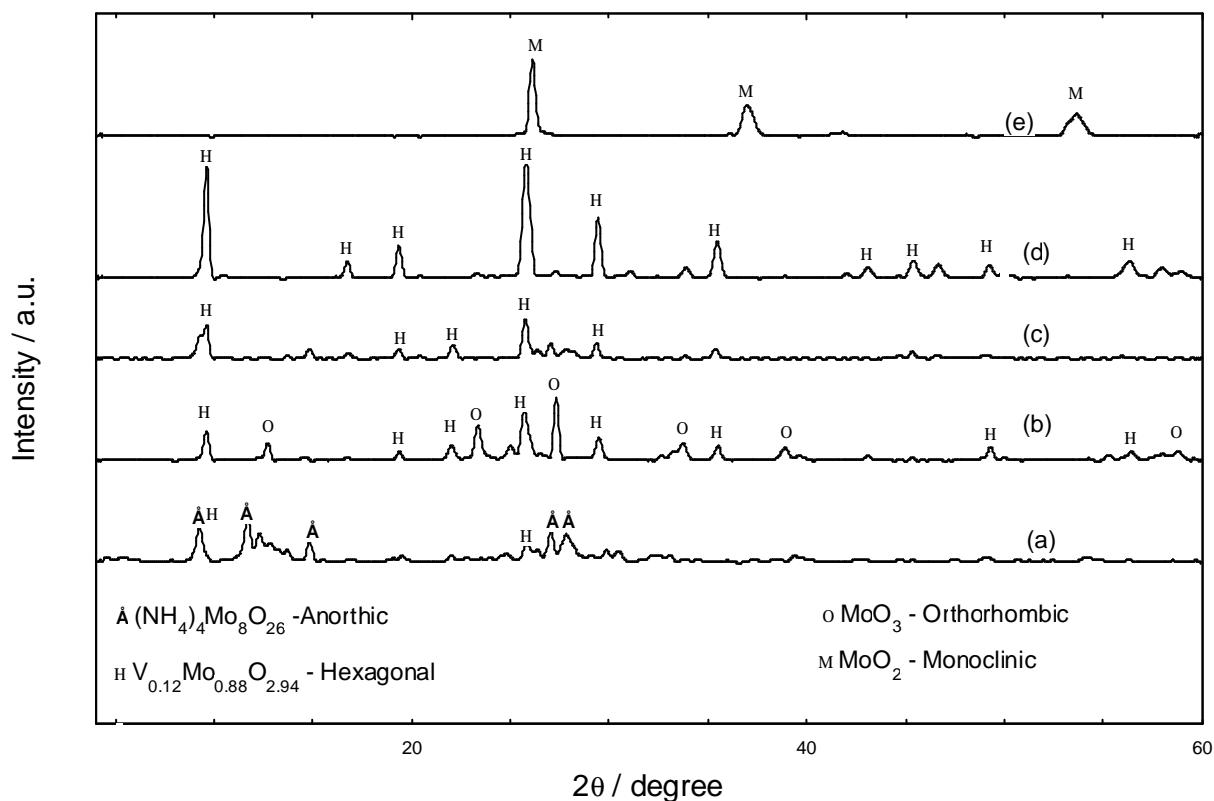


Figure 3: XRD patterns of (a) MoV₅₂₃ (b) MoV₆₂₃ (c) MoV₆₇₃ (d) MoV₇₂₃ and (e) MoV₇₇₃

X-ray diffraction was also carried out for calcined samples. Figure 3 depicts the XRD patterns for the samples calcined at various temperatures. They contain reflection lines of different phases which were found to evolve as the calcinations temperature was increased. For MoV₅₇₃ sample, the presence of anorthic and hexagonal phases are observed. At calcination temperature of 623 K, anorthic phase disappeared and is replaced by the orthorhombic and hexagonal phase. When the sample was calcined at 673 K, orthorhombic phase disappeared and hexagonal phase becomes more prominent. The hexagonal phase becomes significant at higher calcination temperature, i.e. 723 K. However, at 773 K, hexagonal phase disappear and monoclinic phase takes over. The phase changing event is clearly shown from the diffractogram of samples calcined at different temperatures.

BET surface area and particle size

The crystallite size was calculated by the Debye Scherrer equation:

$$t = \frac{0.9 \lambda}{b_{hkl} \times \cos \theta_{hkl}}$$

where t is the crystallite size, λ is 1.5438 Å and b_{hkl} is the FWHM (in radian). Table 1 compiles the BET and particle size results as a function of the calcination temperature. No significant value is observed in the data, only that MoV₆₂₃ shows surface area of only 0.8 m² g⁻¹. This is due to the particles coming together forming bigger particles which reduced the surface area. At this stage, the process of eliminating unwanted species is incomplete which led to the low surface area. In comparison, the higher surface area of the sample calcine at

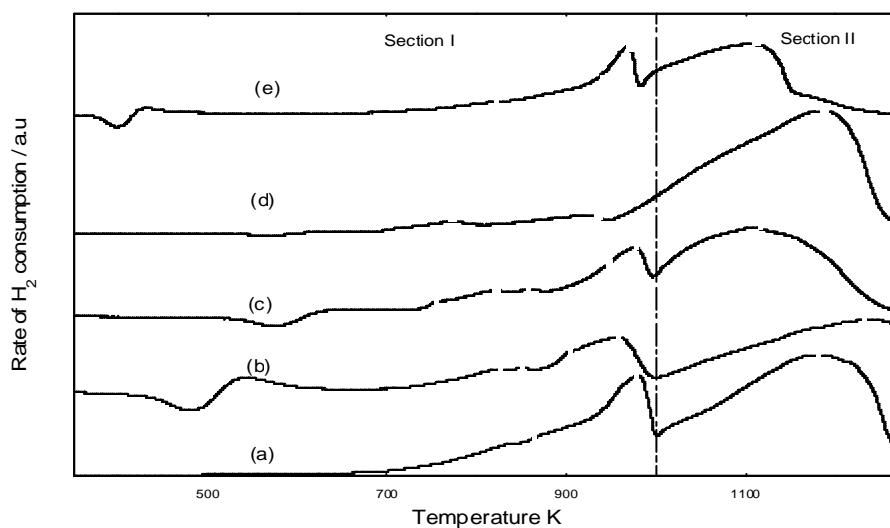
573 K is only contributed by unwanted species. When temperature was increased to 673 K, surface area increased to $3.7 \text{ m}^2 \text{ g}^{-1}$ reckoning that the organic or unwanted species present in the samples have been removed. The surface area value increases to $4.3 \text{ m}^2 \text{ g}^{-1}$ suggesting that at this stage the sample consists of a prominent phase. The value retained at $4.1 \text{ m}^2 \text{ g}^{-1}$, but at this point the phase is not the same as previous ones as evidenced in the diffractograms. For MoV_{573} sample, its surface area of $4.2 \text{ m}^2 \text{ g}^{-1}$ is high but the sample contains the unwanted species which may contribute to high surface area value. There is no clear difference made on crystallite size. One can suggest that crystallite size of the samples fall in the range between 28 to 82 nm.

Table 1: Crystallite size and surface area of MoV_{573} , MoV_{623} , MoV_{673} , MoV_{723} and MoV_{773}

| samples | Crystal system | (hkl) | 2θ (degree) | FWHM | t (nm) | Surface area ($\text{m}^2 \text{ g}^{-1}$) ($\pm 0.05 \text{ m}^2 \text{ g}^{-1}$) |
|----------------------|--|---|-----------------------|--------|----------|--|
| MoV_{573} 1 | $(\text{NH}_4)_4\text{Mo}_8\text{O}_{26}$ -anorthic + | (001) | 9.3 | 0.0974 | 82.0 | 4.2 |
| 2 | | (0-11) | 11.7 | 0.1624 | 49.3 | |
| 3 | | $(\text{V}_{0.12}\text{Mo}_{0.88})\text{O}_{2.94}$ -hexagonal | (201) | 0.1299 | 63.0 | |
| MoV_{623} 1 | $\text{V}_{0.13}\text{Mo}_{0.87}\text{O}_{2.94}$ -hexagonal + | (110) | 23.3 | 0.1624 | 50.0 | 0.8 |
| 2 | | MoO_3 -orthorhombic | (040) | 0.1624 | 50.3 | |
| 3 | | (021) | 27.3 | 0.1299 | 63.1 | |
| MoV_{673} 1 | $\text{V}_{0.13}\text{Mo}_{0.87}\text{O}_{2.94}$ -hexagonal | (100) | 9.6 | 0.0974 | 82.0 | 3.7 |
| 2 | | (210) | 25.7 | 0.1624 | 50.3 | |
| 3 | | (111) | 29.4 | 0.1299 | 63.4 | |
| MoV_{723} 1 | MoO_2 - monoclinic | (100) | 9.7 | 0.0974 | 82.0 | 4.3 |
| 2 | | (210) | 25.7 | 0.1948 | 41.9 | |
| 3 | | (101) | 26.0 | 0.1624 | 50.3 | |
| MoV_{773} 1 | | (011) | 26.1 | 0.1624 | 50.3 | 4.1 |
| 2 | | (-211) | 37.0 | 0.2598 | 32.3 | |
| 3 | | (022) | 53.7 | 0.3168 | 28.2 | |

Temperature Programmed Reduction

Figure 4 shows the TPR profile obtained by passing hydrogen gas in argon stream (5% hydrogen, 1 bar, 25 ml min^{-1}) over the fresh samples.

Figure 4: TPR profile of fresh samples (a) MoV_{573} (b) MoV_{623} (c) MoV_{673} (d) MoV_{723} and (e) MoV_{773}

Profiles can be segmented into section I and section II. In section I, the oxygen removal occurs at many stages as shown by a number of maxima peak. In section II, at least one maximum peak was observed in each sample. Removal of oxygen species in this section is huge based on the larger area under the peak compared to section I. This is probably contributed by the higher temperature of the reduction process which may assist the oxygen bond breakage.

Water evolution occurs as a result of the hydrogen reacting with adsorbed oxygen according to the following reaction:



where (g), (s) is gaseous or surface species and is the oxygen vacancy. An estimate of the amount of oxygen removed by the catalyst in each sample can be made by calculating the area under the peak. The results are shown in Table 2. The reduction activation energies can be obtained from a modified Redhead equation:

$$\frac{E_r}{RT_m^2} = \left[\frac{A_r}{b} \right] [\text{H}_2]_m \exp \left[\frac{-E_r}{RT_m} \right]$$

where T_m is the peak maximum temperature (K) in the rate of production of H_2 , E_r is the reduction activation energy (kcal mol^{-1}), A_r is the reduction pre-exponential term ($\text{cm}^3 \text{mol}^{-1} \text{s}^{-1}$) which is given a standard collision number of $10^{13} \text{ cm}^3 \text{mol}^{-1} \text{s}^{-1}$ and $[\text{H}_2]_m$ is the gas phase concentration of hydrogen (mole cm^{-3}) at the peak maximum.

The values of peak maximum temperature obtained vary from 760 K to 1250 K while the reduction activation energy obtained ranges from $127.1 \text{ kJ mol}^{-1}$ to $207.5 \text{ kJ mol}^{-1}$. These are a very high E_r value, therefore the oxygen may be strongly bonded to the surface of the oxides.

The total number of oxygen atoms removed is 7.1×10^{21} , 5.1×10^{20} , 5.2×10^{21} , 5.8×10^{21} and 7.8×10^{21} atoms g^{-1} for MoV_{573} , MoV_{623} , MoV_{673} , MoV_{723} and MoV_{773} respectively.

Table 2: Reduction activation energy and total number of oxygen removed by reduction in H_2/Ar

| Sample | T_{\max} (K) | Reduction activation energy, $E_r(\text{kJ mol}^{-1})$ | Oxygen removed (mol g^{-1}) ($\pm 1 \times 10^{-8}$) | Oxygen removed (atoms g^{-1}) |
|--------------------|----------------|--|---|---|
| MoV_{573} | 835 | 139.6 | 6.7×10^{-4} | 4.0×10^{20} |
| | 979 | 163.5 | 3.1×10^{-3} | 1.8×10^{21} |
| | 1177 | 196.8 | 8.1×10^{-3} | 4.9×10^{21} |
| | | | 1.2×10^{-2} | 7.1×10^{21} |
| MoV_{623} | 827 | 138.1 | 2.5×10^{-5} | 1.5×10^{19} |
| | 851 | 142.3 | 5.5×10^{-5} | 3.3×10^{19} |
| | 907 | 151.6 | 4.3×10^{-5} | 2.6×10^{19} |
| | 957 | 160.0 | 1.3×10^{-4} | 8.1×10^{19} |
| | 1241 | 207.5 | 5.9×10^{-4} | 3.5×10^{20} |
| | | | 8.4×10^{-4} | 5.1×10^{20} |
| MoV_{673} | 760 | 127.1 | 9.4×10^{-5} | 5.7×10^{19} |
| | 822 | 137.4 | 4.4×10^{-4} | 2.7×10^{20} |
| | 858 | 143.5 | 3.1×10^{-4} | 1.9×10^{20} |
| | 976 | 163.2 | 6.0×10^{-3} | 1.1×10^{21} |
| | 1106 | 184.9 | 1.8×10^{-3} | 3.6×10^{21} |
| | | | 8.6×10^{-3} | 5.2×10^{21} |
| MoV_{723} | 772 | 129.0 | 3.2×10^{-4} | 1.9×10^{20} |
| | 928 | 155.1 | 6.7×10^{-4} | 4.0×10^{20} |
| | 1182 | 197.6 | 8.7×10^{-3} | 5.2×10^{21} |
| | | | 9.7×10^{-3} | 5.8×10^{21} |
| MoV_{773} | 811 | 135.6 | 4.2×10^{-4} | 2.5×10^{20} |
| | 968 | 161.8 | 3.9×10^{-3} | 2.3×10^{21} |
| | 1107 | 185.1 | 8.7×10^{-3} | 5.2×10^{21} |
| | | | 1.3×10^{-2} | 7.8×10^{21} |

Scanning Electron Microscopy

Figure 5 presents the SEM micrographs of MoV₆₇₃ and MoV₇₂₃. Both images exhibit a rather rod-like morphology. There is no dependency of the morphology to the various calcination temperatures imposed. They fully support the tendency understood from the BET and crystallite size measurement.

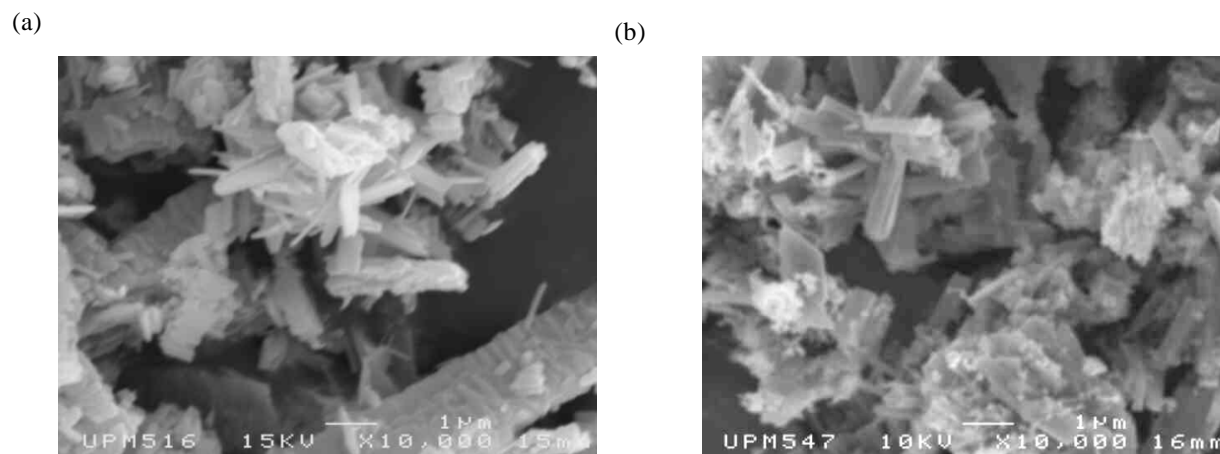


Figure 5: SEM micrographs of (a) MoV₆₇₃ and (b) MoV₇₂₃.

Conclusion

This study establishes the effect of calcination temperature on the physicochemical properties of the MoV mixed oxides, prepared by reflux method. Phase evolution was clearly seen as the temperature was varied. However, the various calcination temperatures were not found to make a huge impact on the morphology of the samples that were rod-like. This was fully supported by the BET and particle size measurements. Also, in TPR study, the samples showed similar reduction behaviour that can be segmented into two sections. Nevertheless, the results did highlight the benefit of the study on various calcination temperatures in order to reach the required active phase.

Acknowledgement

This research is fully supported by the Ministry of Science, Technology and Innovation (MOSTI), Malaysia under EA research scheme. The authors would also like to extend their appreciation to Institute of Bioscience, UPM for allowing electron microscopy to be captured.

References

1. Ueda W., Vitry D. and Katou T. 2004. *Catal. Today* 96: 235-240.
2. Tsuji H. and Koyasu Y. 2001. *JACS Communications* 124: 5608-5609.
3. Adams A.H., Frank H., Buhrmester T., Kunert J., Ott J., Vogel H. and Fuess H. (2004); *J. Mol. Catal. A*:216: 67-74.
4. Tichy J. 1997. *Appl. Catal. A: General* 157: 363-385.
5. Ushikubo T., Oshima K., Kayou A., Vaarkamp M. and Hatano M. 1997. *J.Catal.*:199: 394-396.
6. Kunert J., Drochner A., Ott J., Vogel H. and Fuess H. 2004. *Appl. Catal. A: General* 269: 53-61.